Nontrivial Role of Interlayer Cation States in Iron-Based Superconductors

Daniel Guterding,[1,*] Harald O. Jeschke,[1] I. I. Mazin,[2] J. K. Glasbrenner,[3,†] E. Bascones,[4] and Roser Valentí[1]
[1]Institut für Theoretische Physik, Goethe-Universität Frankfurt, Max-von-Laue-Straße 1, 60438 Frankfurt am Main, Germany
[2]Code 6393, Naval Research Laboratory, Washington, District of Columbia 20375, USA
[3]National Research Council/Code 6393, Naval Research Laboratory, Washington, District of Columbia 20375, USA
[4]Instituto de Ciencia de Materiales de Madrid, ICMM-CSIC, Cantoblanco, 28049 Madrid, Spain
(Received 27 October 2016; published 5 January 2017)

Unconventional superconductivity in iron pnictides and chalcogenides has been suggested to be controlled by the interplay of low-energy antiferromagnetic spin fluctuations and the particular topology of the Fermi surface in these materials. Based on this premise, one would also expect the large class of isostructural and isoelectronic iron germanide compounds to be good superconductors. As a matter of fact, they, however, superconduct at very low temperatures or not at all. In this work we establish that superconductivity in iron germanides is suppressed by strong ferromagnetic tendencies, which surprisingly do not originate from changes in bond angles or bond distances with respect to iron pnictides and chalcogenides, but are due to changes in the electronic structure in a wide range of energies happening upon substitution of atom species (As by Ge and the corresponding spacer cations). Our results indicate that superconductivity in iron-based materials may not always be fully understood based on d or d-p model Hamiltonians only.

DOI: 10.1103/PhysRevLett.118.017204

Introduction.—After the initial discovery of high-temperature superconductivity in doped LaFeAsO [1], a large variety of other iron pnictides and chalcogenides have been shown to be superconductors [2], with some reports of the transition temperature T_c as high as 100 K [3]. On the other hand, isoelectronic and isostructural iron germanides are either nonsuperconducting [4–7] or possibly superconduct at very low temperatures [8,9]. The currently most intensively debated material is YFe_2Ge_2, for which superconductivity below 2 K has been reported [9]. Its electronic structure is similar to that of $CaFe_2As_2$ in the collapsed tetragonal phase, but with significant hole doping [9–11]. This led to speculation [9] about a connection between superconductivity in YFe_2Ge_2 and the collapsed phase of the extremely hole-doped pnictide, KFe_2As_2 [12–14]. Furthermore, Wang *et al.* [15] recently found YFe_2Ge_2 to be close to a magnetic instability and x-ray absorption and photoemission experiments show evidence for strong spin-fluctuations [16] and moderate correlation effects [17] in this material.

Magnetism plays an important role in superconductivity of Fe-based superconductors (FeBS) [2,18–24]. It is therefore natural to ask whether the magnetic tendencies in iron germanides are fundamentally different from those in iron pnictides and chalcogenides [25] and why that is the case. In a first attempt to understand the lack of superconductivity in Fe germanides, a few authors investigated the electronic properties of the isoelectronic and isostructural materials MgFeGe and LiFeAs [26–28]. The former is a paramagnetic metal, while the latter is a superconductor. An important conclusion was that the dominant magnetic exchange interactions in MgFeGe are ferromagnetic, while those in LiFeAs are antiferromagnetic. The microscopic origin of this different behavior was, however, not further explored.

In this Letter we show that (i) the presence of ferromagnetic tendencies is a general trait in iron germanides, which is detrimental for superconductivity, and that (ii) the ferromagnetic tendencies arise from the interaction of the cation spacer with the FeGe layer. In fact, the hole-doping or collapse of the c axis in YFe_2Ge_2 are not essential for this behavior, but the key is in the substitution of As by Ge and the corresponding substitution of monovalent or divalent spacers by divalent or trivalent cations, respectively. This modifies the electronic band structure in a wide range of energies at and away from the Fermi level and creates ferromagnetic tendencies which suppress superconductivity. Hence, one can go from As to Se/Te, i.e., right in the periodic table, and find further FeBS, but not to the left towards Ge. In agreement with recent NMR measurements [29], our study highlights the role of the presence or absence of ferromagnetic fluctuations in determining the value of T_c in FeBS.

Our analysis shows that conventional low-energy models of FeBS, which only incorporate the Fe d and X (X = As, Se, Ge, ...) p states are in some cases not sufficient to explain key features of FeBS. Although these models usually reproduce the Fermi surface very well, they do not reflect the physical instabilities of the actual materials because they neglect the interaction with the spacer between the FeX layers. Even though bulk FeSe does not contain spacer layers, our arguments may be relevant for intercalates [30–32], alkali-dosed thick films [33], and FeSe monolayers on $SrTiO_3$ [3].

Materials and methods.—We compare isoelectronic iron arsenides and iron germanides from (i) the so-called

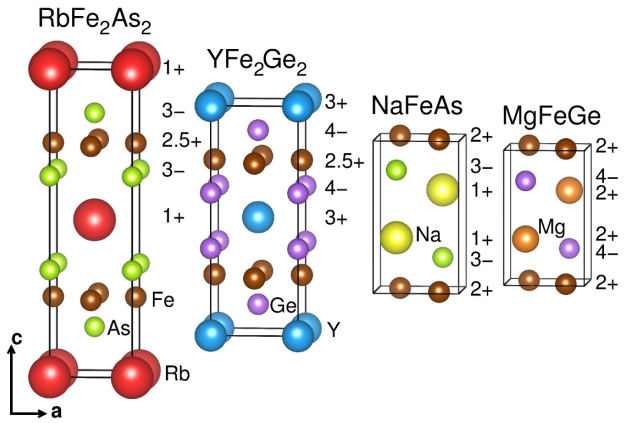

FIG. 1. Crystal structures of $RbFe_2As_2$, YFe_2Ge_2, NaFeAs, and MgFeGe. The unit cells and interatomic distances are true to scale. The numbers next to the unit cells indicate the nominal valence of atoms at the same vertical positions.

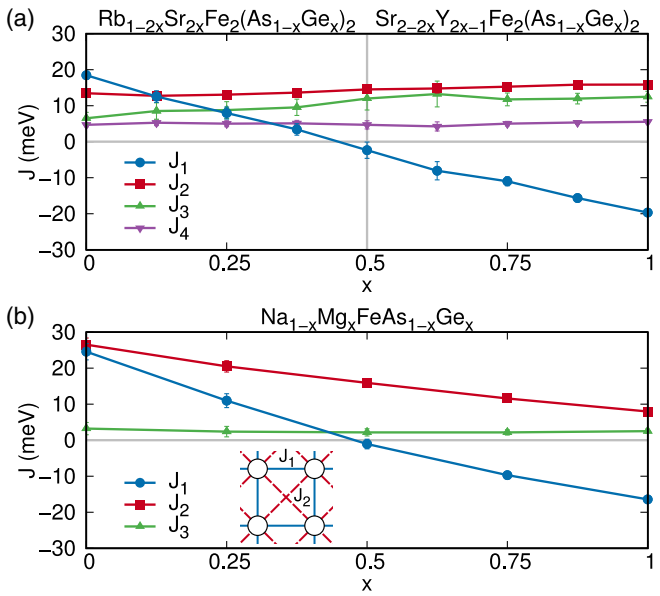

FIG. 2. Calculated Heisenberg exchange parameters for (a) the VCA interpolation between $RbFe_2As_2$ and YFe_2Ge_2 [via $SrFe_2(As_{0.5}Ge_{0.5})_2$] and (b) the VCA interpolation between NaFeAs and MgFeGe. Lines are guides to the eye. The error bars represent the statistical errors of the fit. The inset of (b) shows the structure of the two-dimensional Heisenberg model we use to fit the DFT energies. J_1 is the nearest-neighbor coupling in the square lattice of Fe atoms, while J_2 is the next-nearest neighbor coupling. J_3 and J_4 are longer-range exchange couplings. Positive values of J correspond to antiferromagnetic exchange. Note that all calculations were performed in the crystal structures of YFe_2Ge_2 and MgFeGe, respectively.

hole-doped 122 family where iron is in a nominal oxidation $Fe^{2.5+}$ with $d^{5.5}$ occupation [34–36] and (ii) the so-called 111 family with Fe^{2+} in a d^6 configuration [36–38]. The crystal structures of $RbFe_2As_2$, YFe_2Ge_2, NaFeAs, and MgFeGe are shown in Fig. 1, where we also indicate the nominal valences of the atoms in each compound. Lattice constants and internal positions in this figure were taken from experiment [7,39–41].

The most obvious structural difference between iron arsenides and iron germanides is the shrinking of the c axis (Fig. 1). From NaFeAs to MgFeGe it is not as pronounced as from $RbFe_2As_2$ to YFe_2Ge_2, where Ge p_z-p_z bonds may form (in MgFeGe direct Ge-Ge bonding is not possible). Although these materials are isoelectronic, the germanides have a stronger charge transfer between the FeX (X = As, Ge) and the spacer layers.

The isoelectronic substitution of As by Ge, Rb by Y, and Na by Mg was simulated within the virtual crystal approximation (VCA). To disentangle effects originating from direct atomic substitution from effects coming from small changes of bond distances and angles in real materials, we performed all calculations for the 122 family with the experimental structural parameters of YFe_2Ge_2 [39] and those for the 111 family with the experimental structural parameters of MgFeGe [7]. The technical details of our DFT calculations can be found in Ref. [42].

We also analyze the density of states by using the extended Stoner model [45,46], which is a simple tool for understanding the origin of itinerant ferromagnetism (see Ref. [42] for details). The paramagnetic state is unstable towards ferromagnetism if the conditions $1/I = \bar{N}(m)$ and $0 > d\bar{N}(m)/dm$ are fullfilled at some m, where $\bar{N}(m)$ is the paramagnetic density of states averaged over an energy window that contains a sufficient number of states to realize an Fe moment m, and I is the Stoner parameter [42].

Results.—We first calculated the DFT energies of various spin configurations. By means of the VCA we interpolated between $RbFe_2As_2$ and YFe_2Ge_2 [via $SrFe_2(As_{0.5}Ge_{0.5})_2$] and between NaFeAs and MgFeGe. Using a two-dimensional Heisenberg model to parameterize the DFT energies (see Ref. [42] for more details), we observe that the nearest-neighbor exchange coupling J_1 universally changes from antiferromagnetic to ferromagnetic when going continuously from As to Ge without changing the electron count, while all other exchange couplings are almost unaffected (Fig. 2). Only in the 111 family the next-nearest-neighbor exchange J_2 is also reduced, but it does not change sign. At the germanide end point the ferromagnetic J_1 becomes the dominant exchange interaction.

Remarkably, we also obtained a large ferromagnetic J_1 for NaFeAs after we expanded the structure used for Fig. 2 by 10% along the c axis but kept all distances within the FeAs layer unchanged by the expansion. These results indicate that NaFeAs can also be turned ferromagnetic by separating the FeAs layers and by shifting Na further away from the layers.

From this analysis we conclude that previous suggestions [15] that iron germanides and iron pnictides show similar magnetic behavior do not hold. While both families

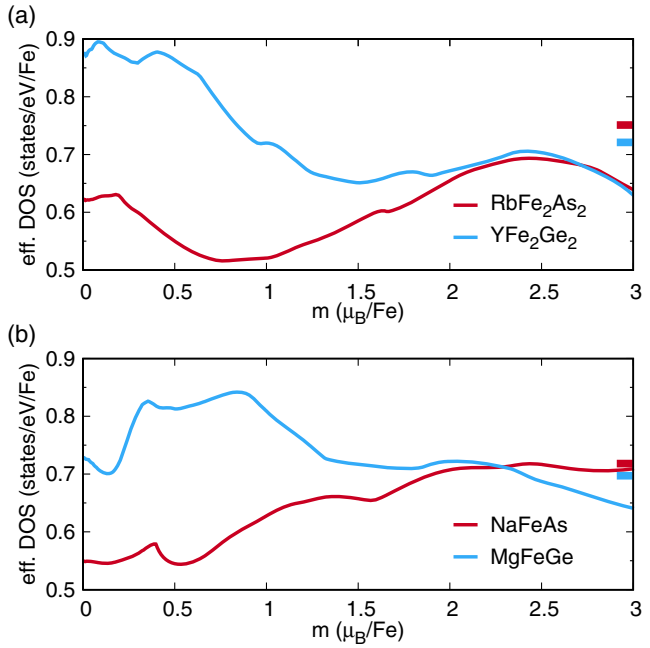

FIG. 3. Effective density of states in the extended Stoner model as a function of magnetic moment for (a) $RbFe_2As_2$ and YFe_2Ge_2 and (b) NaFeAs and MgFeGe. The colored bars on the right y axis indicate the calculated inverse Stoner parameters $1/I$ for the respective case. All calculations were performed in the crystal structures of YFe_2Ge_2 and MgFeGe, respectively.

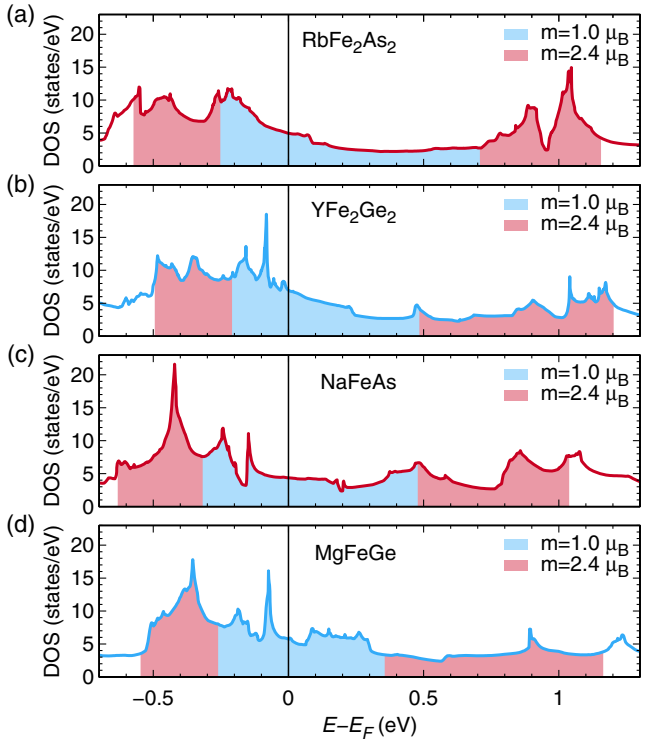

FIG. 4. Total density of states calculated from DFT for (a) $RbFe_2As_2$, (b) YFe_2Fe_2, (c) NaFeAs, and (d) MgFeGe. The shaded areas below the curves correspond to the energy range needed to realize a moment of $1.0\mu_B$ or $2.4\mu_B$ per iron, respectively, within the extended Stoner model. All calculations were performed in the crystal structures of YFe_2Ge_2 and MgFeGe, respectively.

have a stripe antiferromagnetic ground state in the DFT calculations, the nature of excitations is entirely different. This is reflected in the presence of a nearest neighbor ferromagnetic exchange J_1 in iron germanides and antiferromagnetic J_1 in the iron pnictides despite the very similar crystal structure and electronic structure at the Fermi level. In particular, the results on the expanded NaFeAs suggest that the origin of this different behavior lies dominantly in the relative separation between the spacer and the FeX plane.

A further distinctive feature of the germanides is that the magnetism of Fe in YFe_2Ge_2 appears to be rather peculiar. There is a low- and a high-moment solution for Fe, the former more stabilized for shorter Fe-Ge bond lengths [42] (in pnictides, either a high-spin solution is realized, or magnetism collapses completely).

To understand in a simple framework the origin of the magnetic behavior presented above, we investigate the effective density of states $\bar{N}$ as a function of the magnetic moment m within the extended Stoner model (see Fig. 3). We observe that (i) iron germanides have, in general, a higher DOS at the Fermi level and (ii) a significant number of states is shifted from higher energies towards the Fermi level, as compared to pnictides. This is signaled by the strong increase of the effective DOS at low moments (see Fig. 3 where results for YFe_2Ge_2 vs $RbFe_2As_2$ and MgFeGe vs NaFeAs are shown). Interestingly, the changes in the high-moment region ($m \sim 2.4\mu_B$) are marginal, while they are considerable in the low-moment region ($m < 1.0\mu_B$). Furthermore, we find that the Stoner parameter I is almost independent of the material and that $1/I$ lies between 0.7 and 0.75 eV^{-1}. Therefore, by looking for crossings of $\bar{N}(m)$ with $1/I$ in Fig. 3, we establish that the extended Stoner criterion for ferromagnetism is fulfilled in iron germanides, but not in pnictides. Moreover, the metastability of different magnetic moments in YFe_2Ge_2 is also evident from this analysis, as the effective DOS almost fulfills the extended Stoner criterion also for large moments of about $2.5\mu_B$.

Figure 4 shows the total calculated DOS for $RbFe_2As_2$ vs YFe_2Ge_2 and NaFeAs vs MgFeGe, where we colored the energy regions corresponding to magnetic moments of $m = 1.0\mu_B$ (blue) and $m = 2.4\mu_B$ (red) in the extended Stoner model. The energy range corresponding to $m = 1.0\mu_B$ is compressed when going from arsenides to germanides, while the energy range corresponding to $m = 2.4\mu_B$ increases marginally in germanides. As the density of states in the window shown is dominated by Fe states, this implies that the bandwidth of some of the Fe states is selectively reduced in iron germanides, while the overall bandwidth is about constant [42].

Discussion.—One of the principal questions in the theory of the Fe-based superconductors is what should be the minimal chemical model to explain the essential physics and, above all, superconductivity. It was recognized that the effective Fe-only ("*d*-only") model does not work in some materials, but it has been believed so far that the electronic properties of iron-based superconductors were exclusively controlled by the FeX layers (X = As, Se, Ge, ...) as described by the so-called "*d*-*p* model". Thereby the role of all other constituents was reduced to charge reservoirs.

We have established in this work that iron germanides have a general tendency towards ferromagnetism which proves detrimental for superconductivity, even though the Fermi surface is very similar to that of isoelectronic pnictides. Most importantly, this tendency can be traced down to the flattening of some bands near the Fermi level and a modified electronic band structure in a wide range of energies at and away from the Fermi level. Neither the collapse of the c axis, nor the hole doping of the 122 germanides are essential for the emergence of ferromagnetism. However, the character and position of the intercalating species, normally considered irrelevant and not explicitly included in any theory or model, plays a decisive role.

Our findings have important implications for iron-based superconductivity in general. (i) The Fermi surface geometry and topology is an important, but not the only condition for emerging superconductivity. The character of spin fluctuations, even on the level of the simple ferromagnetic-antiferromagnetic dichotomy, may be qualitatively different in seemingly similar materials. (ii) A quantitative theory of T_c in iron-based superconductors must include the interaction between all constituents of the unit cell, including, in some cases, the interlayer spacers. (iii) While FeGe layers *per se* are not necessarily ferromagnetic, the fact that they have to be spaced with different elements (e.g., Mg vs Na, or Y vs Sr) drives them ferromagnetic. (iv) In a more general way, it does matter what we place next to or on top of an Fe-ligand layer. This observation may be directly related to an apparent role that interfacial effects play in high-T_c Fe chalcogenides, such as FeSe monolayers deposited on specially prepared surfaces or $K_xFe_{2-y}Se_2$ filaments embedded in the magnetic $K_2Fe_4Se_5$ phase.

D. G., H. O. J., and R. V. thank the German Research Foundation (Deutsche Forschungsgemeinschaft) for financial support through grant SPP 1458. I. I. M. was supported by ONR through the NRL basic research program and by the Alexander von Humboldt Foundation. J. K. G. acknowledges the support of the NRC program at NRL. E. B. acknowledges funding from Ministerio de Economía y Competitividad vía Grant No. FIS2014-53219-P and from Fundación Ramón Areces and thanks R. Rurali and X. Cartoixa for early calculations. The authors thank S. L. Bud'ko and P. C. Canfield for helpful discussions.

*guterding@itp.uni-frankfurt.de
†Present address: Department of Computational and Data Sciences and Computational Materials Science Center, George Mason University, 4400 University Drive, Fairfax, VA 22030, USA.

[1] Y. Kamihara, T. Watanabe, M. Hirano, and H. Hosono, Iron-based layered superconductor La$[O_{1-x}F_x]$FeAs (x = 0.05-0.12) with T_c = 26 K, J. Am. Chem. Soc. **130**, 3296 (2008).

[2] H. Hosono and K. Kuroki, Iron-based superconductors: Current status of materials and pairing mechanism, Physica (Amsterdam) **514C**, 399 (2015).

[3] J.-F. Ge, Z.-L. Liu, C. Liu, C.-L. Gao, D. Qian, Q.-K. Xue, Y. Liu, and J.-F. Jia, Superconductivity above 100 K in single-layer FeSe films on doped $SrTiO_3$, Nat. Mater. **11**, 285 (2015).

[4] M. A. Avila, S. L. Bud'ko, and P. C. Canfield, Anisotropic magnetization, specific heat and resistivity of RFe_2Ge_2 single crystals, J. Magn. Magn. Mater. **270**, 51 (2004).

[5] S. Ran, S. L. Bud'ko, and P. C. Canfield, Effects of substitution on low-temperature physical properties of $LuFe_2Ge_2$, Philos. Mag. **91**, 4388 (2011).

[6] H. Kim, S. Ran, E. D. Mun, H. Hodovanets, M. A. Tanatar, R. Prozorov, S. L. Bud'ko, and P. C. Canfield, Crystal growth and annealing study of fragile, non-bulk superconductivity in YFe_2Ge_2, Philos. Mag. **95**, 804 (2015).

[7] X. Liu, S. Matsuishi, S. Fujitsu, and H. Hosono, MgFeGe is an isoelectronic and isostructural analog of the superconductor LiFeAs, Phys. Rev. B **85**, 104403 (2012).

[8] Y. Zou, Z. Feng, P. W. Logg, J. Chen, G. Lampronti, and F. M. Grosche, Fermi liquid breakdown and evidence for superconductivity in YFe_2Ge_2, Phys. Status Solidi RRL **8**, 928 (2014).

[9] J. Chen, K. Semeniuk, Z. Feng, P. Reiss, P. Brown, Y. Zou, P. W. Logg, G. I. Lampronti, and F. M. Grosche, Unconventional Superconductivity in the Layered Iron Germanide YFe_2Ge_2, Phys. Rev. Lett. **116**, 127001 (2016).

[10] A. Subedi, Unconventional sign-changing superconductivity near quantum criticality in YFe_2Ge_2, Phys. Rev. B **89**, 024504 (2014).

[11] D. J. Singh, Superconductivity and magnetism in YFe_2Ge_2, Phys. Rev. B **89**, 024505 (2014).

[12] J.-J. Ying, L.-Y. Tang, V. V. Struzhkin, H.-K. Mao, A. G. Gavriulik, A.-F. Wang, X.-H. Chen, and X.-J. Chen, Tripling the critical temperature of KFe_2As_2 by carrier switch, arXiv:1501.00330.

[13] Y. Nakajima, R. Wang, T. Metz, X. Wang, L. Wang, H. Cynn, S. T. Weir, J. R. Jeffries, and J. Paglione, High-temperature superconductivity stabilized by electron-hole interband coupling in collapsed tetragonal phase of KFe_2As_2 under high pressure, Phys. Rev. B **91**, 060508 (R) (2015).

[14] D. Guterding, S. Backes, H. O. Jeschke, and R. Valentí, Origin of the superconducting state in the collapsed tetragonal phase of KFe_2As_2, Phys. Rev. B **91**, 140503(R) (2015).

[15] G. Wang and X. Shi, Electronic strctures and magnetism of YM_2Ge_2 (M = Mn-Cu): Ge-height dependent magnetic ordering in YFe_2Ge_2, Comput. Mater. Sci. **121**, 48 (2016).

[16] N. Sirica, F. Bondino, S. Nappini, I. Píš, L. Poudel, A. D. Christianson, D. Mandrus, D. J. Singh, and N. Mannella,

Spectroscopic evidence for strong quantum spin fluctuations with itinerant character in YFe_2Ge_2, Phys. Rev. B **91**, 121102(R) (2015).

[17] D. F. Xu, D. W. Shen, D. Zhu, J. Jiang, B. P. Xie, Q. S. Wang, B. Y. Pan, P. Dudin, T. K. Kim, M. Hoesch, J. Zhao, X. G. Wan, and D. L. Feng, Electronic structure of YFe_2Ge_2 studied by angle-resolved photoemission spectroscopy, Phys. Rev. B **93**, 024506 (2016).

[18] P. J. Hirschfeld, M. M. Korshunov, and I. I. Mazin, Gap symmetry and structure of Fe-based superconductors, Rep. Prog. Phys. **74**, 124508 (2011).

[19] A. Chubukov, Pairing Mechanism in Fe-Based Superconductors, Annu. Rev. Condens. Matter Phys. **3**, 57 (2012).

[20] J. C. S. Davis and D.-H. Lee, Concepts relating magnetic interactions, intertwined electronic orders, and strongly correlated superconductivity, Proc. Natl. Acad. Sci. U.S.A. **110**, 17623 (2013).

[21] J. K. Glasbrenner, I. I. Mazin, H. O. Jeschke, P. J. Hirschfeld, R. M. Fernandes, and R. Valentí, Effect of magnetic frustration on nematicity and superconductivity in Fe chalcogenides, Nat. Phys. **11**, 953 (2015).

[22] Q. Si, R. Yu, and E. Abrahams, High-temperature superconductivity in iron pnictides and chalcogenides, Nat. Rev. Mater. **1**, 16017 (2016).

[23] J. Hu, Identifying the genes of unconventional high temperature superconductors, Science bulletin **61**, 561 (2016).

[24] D. Guterding, S. Backes, M. Tomić, H. O. Jeschke, and R. Valentí, *Ab initio* perspective on structural and electronic properties of iron-based superconductors, arXiv:1606.04411 [Phys. Status Solidi B (to be published)].

[25] E. Bascones, B. Valenzuela, and M. J. Calderón, Magnetic interactions in iron superconductors: A review, C.R. Phys. **17**, 36 (2016).

[26] H. O. Jeschke, I. I. Mazin, and R. Valentí, Why MgFeGe is not a superconductor, Phys. Rev. B **87**, 241105(R) (2013).

[27] Z. P. Yin, K. Haule, and G. Kotliar, Spin dynamics and orbital-antiphase pairing symmetry in iron-based superconductors, Nat. Phys. **10**, 845 (2014).

[28] M.-C. Ding and Y.-Z. Zhang, Possible way to turn MgFeGe into an iron-based superconductor, Phys. Rev. B **89**, 085120 (2014).

[29] P. Wiecki, B. Roy, D. C. Johnston, S. L. Bud'ko, P. C. Canfield, and Y. Furukawa, Competing Magnetic Fluctuations in Iron Pnictide Superconductors: Role of Ferromagnetic Spin Correlations Revealed by NMR, Phys. Rev. Lett. **115**, 137001 (2015).

[30] M. Burrard-Lucas, D. G. Free, S. J. Sedlmaier, J. D. Wright, S. J. Cassidy, Y. Hara, A. J. Corkett, T. Lancaster, P. J. Baker, S. J. Blundell, and S. J. Clarke, Enhancement of the superconducting transition temperature of FeSe by intercalation of a molecular spacer layer, Nat. Mater. **12**, 15 (2013).

[31] D. Guterding, H. O. Jeschke, P. J. Hirschfeld, and R. Valentí, Unified picture of the doping dependence of superconducting transition temperatures in alkali metal/ammonia intercalated FeSe, Phys. Rev. B **91**, 041112(R) (2015).

[32] H. Sun, D. N. Woodruff, S. J. Cassidy, G. M. Allcroft, S. J. Sedlmaier, A. L. Thompson, P. A. Bingham, S. D. Forder, S. Cartenet, N. Mary, S. Ramos, F. R. Foronda, B. J. Williams, X. Li, S. J. Blundell, and S. J. Clarke, Soft Chemical Control of Superconductivity in Lithium Iron Selenide Hydroxides $Li_{1-x}Fe_x(OH)Fe_{1-y}Se$, Inorg. Chem. **54**, 1958 (2015).

[33] C. H. P. Wen, H. C. Xu, C. Chen, Z. C. Huang, X. Lou, Y. K. Pu *et al.*, Anomalous correlation effects and unique phase diagram of electron-doped FeSe revealed by photoemission spectroscopy, Nat. Commun. **7**, 10840 (2016).

[34] S. Backes, D. Guterding, H. O. Jeschke, and R. Valentí, Electronic structure and de Haas-van Alphen frequencies in KFe_2As_2 within LDA+DMFT, New J. Phys. **16**, 083025 (2014).

[35] S. Backes, H. O. Jeschke, and R. Valentí, Microscopic nature of correlations in multi-orbital AFe_2As_2 ($A = $ K, Rb, Cs): Hund's coupling versus Coulomb repulsion, Phys. Rev. B **92**, 195128 (2015).

[36] Z. P. Yin, K. Haule, and G. Kotliar, Kinetic frustration and the nature of the magnetic and paramagnetic states in iron pnictides and iron chalcogenides, Nat. Mater. **10**, 932 (2011).

[37] J. Ferber, K. Foyevtsova, R. Valentí, and H. O. Jeschke, LDA+DMFT study of the effects of correlation in LiFeAs, Phys. Rev. B **85**, 094505 (2012).

[38] G. Lee, H. S. Ji, Y. Kim, C. Kim, K. Haule, G. Kotliar, B. Lee, S. Khim, K. H. Kim, K. S. Kim, K.-S. Kim, and J. H. Shim, Orbital Selective Fermi Surface Shifts and Mechanism of High Tc Superconductivity in Correlated *A*FeAs (A = Li, Na), Phys. Rev. Lett. **109**, 177001 (2012).

[39] G. Venturini and B. Malaman, X-ray single crystal refinements on some RT_2Ge_2 compounds ($R = $ Ca,Y,La,Nd,U; $T = $ Mn-Cu, Ru-Pd): evolution of the chemical bonds, J. Alloys Compd. **235**, 201 (1996).

[40] D. R. Parker, M. J. Pitcher, P. J. Baker, I. Franke, T. Lancaster, S. J. Blundell, and S. J. Clarke, Structure, antiferromagnetism and superconductivity of the layered iron arsenide NaFeAs, Chem. Commun. **16**, 2189 (2009).

[41] F. Eilers, K. Grube, D. A. Zocco, T. Wolf, M. Merz, P. Schweiss, R. Heid, R. Eder, R. Yu, J.-X. Zhu, Q. Si, T. Shibauchi, and H. v. Löhneysen, Strain-Driven Approach to Quantum Criticality in AFe_2As_2 with $A = $ K, Rb, and Cs, Phys. Rev. Lett. **116**, 237003 (2016).

[42] See Supplemental Material at http://link.aps.org/supplemental/10.1103/PhysRevLett.118.017204, which provides additional information on the metastability of magnetic moments, details of the extended Stoner analysis, and electronic band structures with orbital weights for the VCA calculation, including Refs. [43] and [44].

[43] K. Koepernik and H. Eschrig, Full-potential nonorthogonal local-orbital minimum-basis band-structure scheme, Phys. Rev. B **59**, 1743 (1999); http://www.FPLO.de.

[44] J. P. Perdew, K. Burke, and M. Ernzerhof, Generalized Gradient Approximation Made Simple, Phys. Rev. Lett. **77**, 3865 (1996).

[45] O. K. Andersen, J. Madsen, U. K. Poulsen, O. Jepsen, and J. Kollár, Magnetic ground state properties of transition metals, Physica (Amsterdam) **86–88B+C**, 249 (1977).

[46] I. I. Mazin and D. J. Singh, Electronic structure and magnetism in Ru-based perovskites, Phys. Rev. B **56**, 2556 (1997).